

Near-Edge X-ray Absorption Fine Structure Spectroscopy of MDI and TDI Polyurethane Polymers

Stephen G. Urquhart,^{*,†} Archie P. Smith,[†] Harald W. Ade,[†] Adam P. Hitchcock,[‡]
Edward G. Rightor,[§] and Werner Lidy^{||}

Department of Physics, North Carolina State University, Raleigh, North Carolina, 27695-8202,
Brockhouse Institute for Materials Research, McMaster University, Hamilton, ON, L8S 4M1, Canada,
Dow Chemical USA, Midland, Michigan, 48667, and Dow Chemical USA, Freeport, Texas, 77541

Received: January 5, 1999; In Final Form: March 31, 1999

The sensitivity of near-edge X-ray absorption fine structure (NEXAFS) to differences in key chemical components of polyurethane polymers is presented. Carbon 1s NEXAFS spectra of polyurethane polymers made from 4,4'-methylene di-*p*-phenylene isocyanate (MDI) and toluene diisocyanate (TDI) isocyanate monomers illustrate that there is an unambiguous spectroscopic fingerprint for distinguishing between MDI-based and TDI-based polyurethane polymers. NEXAFS spectra of MDI and TDI polyurea and polyurethane models show that the urea and carbamate (urethane) linkages in these polymers can be distinguished. The NEXAFS spectroscopy of the polyether component of these polymers is discussed, and the differences between the spectra of MDI and TDI polyurethanes synthesized with polyether polyols of different molecular composition and different molecular weight are presented. These polymer spectra reported herein provide appropriate model spectra to represent the pure components for quantitative microanalysis.

1. Introduction

Polyurethane polymers are a versatile class of materials with a wide range of applications, including upholstery, carpet-backing, and automotive trim. The desire to make polyurethane foams with better mechanical properties, such as improved tensile-tear resistance, compression set, and durability, drives present research in polyurethane chemistry and formulation. The mechanical properties of polyurethane foams are dependent on both the macroscopic foam cell geometry and the morphology of the polymer contained in the foam's structural elements.¹ This morphology is driven by micro- and macrophase segregation during the polymerization reaction and by the inclusion of fillers such as copolymer particles.² To understand the nature of the phase segregation directly, chemically sensitive, spatially resolved probes of polymer microstructure are required. Scanning transmission X-ray microscopy (STXM) is well suited to this problem. In the STXM microscope, micrographs can be acquired using an X-ray photon energy that corresponds to a chemically sensitive core electron electronic transition, or X-ray absorption spectra can be acquired from spatially resolved 0.01 μm^2 regions. These near-edge X-ray absorption fine structure (NEXAFS) spectromicroscopy techniques are analogous to energy-filtered TEM imaging³ and electron energy loss spectroscopy in a transmission electron microscope (TEM-EELS).⁴ A discussion of the relative merits of STXM versus TEM-EELS spectroscopy for polymers has been presented previously.⁵ Relative to TEM-EELS, STXM spectromicroscopy can acquire spectra with relatively low radiation damage and high spectral energy resolution but lower spatial resolution (~ 35 nm in ideal samples).

This paper explores the sensitivity of NEXAFS spectra to the chemical structure of polyurethane polymers. The unique spectral "fingerprints" of polyurethane polymers made with different formulations—different aromatic isocyanate monomers, different types of polyether, different polyether concentrations, and differing urea/carbamate (urethane) content—are documented and discussed. Understanding the NEXAFS spectra of polyurethane polymer components is required to explore the morphology and chemistry of polyurethane polymers using STXM.

We have previously used TEM-EELS spectroscopy to examine the core excitation spectra of model methylene di-*p*-phenylene isocyanate (MDI) polyurethane polymers,⁶ in comparison to calculations and gas-phase inner-shell electron energy loss spectroscopy (ISEELS) studies of small molecules that are structural analogues to these polyurethane structures.⁷ That work demonstrated that core excitation spectroscopy can distinguish urea and carbamate (urethane) functional groups and established an empirical baseline for understanding the sensitivity of core excitation spectroscopy of polyurethanes. This study extends this earlier work to a wider range of polymers, using the higher resolution NEXAFS spectroscopy to achieve an enhanced chemical sensitivity.

High chemical sensitivity is demanded from these spectroscopy techniques, as the reaction chemistry of polyurethanes is complex because of side reactions and many process variables. The basic chemistry of flexible polyurethane foams consists of three major reagents: an aromatic diisocyanate (OCN-Ar-NCO), a polyether polyol (HO-R-OH), and water. The reaction of an isocyanate group and the polyether polyol -OH group forms a carbamate linkage (Ar-NH-C(O)-O-R). The reaction of two isocyanate groups with water forms a urea linkage (Ar-NH-C(O)-NH-Ar) and CO₂ gas; this gas "blows" the foam. Two types of diisocyanates are typically used for polyurethane foams: toluene diisocyanate (TDI) and MDI.

[†] North Carolina State University.

[‡] McMaster University.

[§] Dow Chemical USA, Midland, Michigan.

^{||} Dow Chemical USA, Freeport, Texas.

TDI-based flexible foams predominate in North America, while MDI is the basis for flexible foams in Europe because of different history, demands of the marketplace, etc. The polyether polyol is varied to optimize the physical properties of the foam: poly(propylene oxide) (PPO) versus poly(ethylene oxide) (PEO) polyethers; di- or trifunctionality; secondary or primary $-OH$; and differing molecular weights. Therefore, the ideal chemically sensitive probe must be able to distinguish urea and carbamate linkages, quantify the polyether content, and identify the type of diisocyanate used (MDI versus TDI). We demonstrate all of these capabilities in the present work. The complications inherent to applying this spectroscopic information to the chemical microanalysis of "real" polyurethane materials, including the role of sample damage and the presence of minority components, will be presented elsewhere.^{2,8}

In this study, we compare the NEXAFS spectra of polyurethane polymers made with the two most common diisocyanate monomers: MDI and TDI. This is the first report of the NEXAFS spectra of TDI-based polyurethane polymers and NEXAFS comparison of polymers containing urea and carbamate functional groups. We evaluate the ability of NEXAFS to distinguish urea and carbamate linkages and its sensitivity to this distinction when these linkages are present in polyurethanes that have a high polyether concentration. A comparison is made to the set of MDI polymer spectra previously acquired by TEM-EELS⁶ to demonstrate the improved chemical sensitivity that results from the higher spectral resolution of these NEXAFS spectra. Molecular model spectra, acquired by ISEELS, are used to aid the assignment of the polymer spectra. The present results for the TDI model polymers are used as reference standards for quantitative functional group compositional analysis elsewhere.⁸

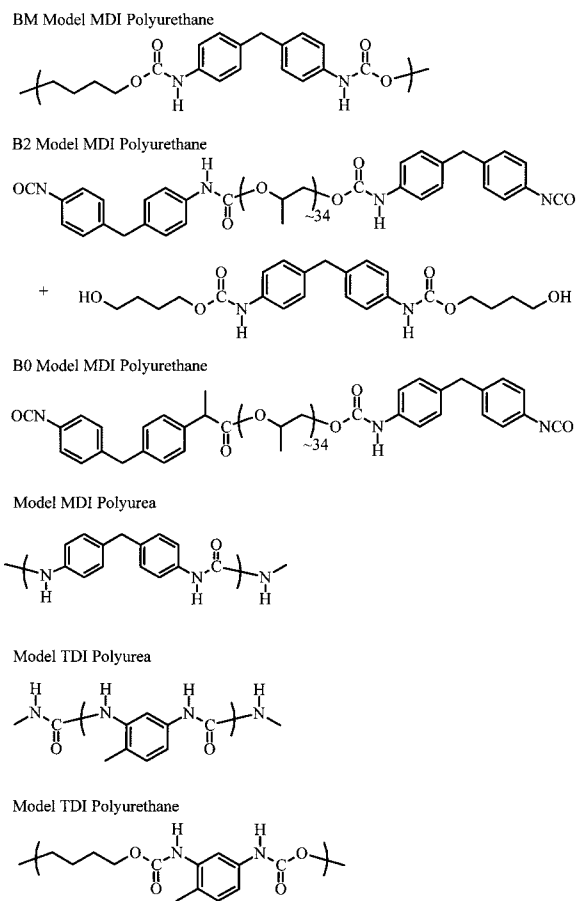
2. Experimental Section

2.1. Materials. Chart 1 presents the structures of the model polyurethane polymers that are the subject of this paper. These polymers were chosen to isolate particular chemical environments present in complex polyurethane polymers. These models represent polymers made with the two most common diisocyanate monomers—MDI and TDI (mixed isomers: 80% 2,4 TDI; 20% 2,6 TDI).

The MDI polymers B2 and B0 were prepared as part of a previous multitechnique study,⁹ and the original sample labels are used here. The B2 polymer is formed by the reaction of a soft-segment prepolymer (OCN-X-NCO) and a hard segment prepolymer (HO-Y-OH) (see Chart 1 for identity of X, Y units). The soft segment prepolymer is a 2000 MW poly(propylene oxide) diol (approximately 34 PPO repeat units) capped by MDI, and the hard segment prepolymer is MDI capped by butane diol. The B0 polymer model is the prepolymer OCN-X-NCO that was used for the synthesis of B2. The BM polymer was prepared by the reaction of MDI with an excess of butane diol under similar conditions as B2 and B0. The B2, BM, and the MDI polyurea polymers are solid, while the B0 species is a viscous liquid. BM is aromatic or "hard segment" rich polymer, B0 is "soft segment" or polyether rich, while B2 has an intermediate composition.

The TDI polymers were made with an 80:20 mixture of 2,4- and 2,6-isomers of the monomer toluene diisocyanate. This is the same isomeric composition used in the commercial TDI polyurethanes that we wish to model. The model TDI polyurethane polymer was formed from the reaction of TDI with butane diol. The model TDI polyurea polymer was prepared by dropping small amounts of TDI onto liquid-distilled water and

CHART 1^a



^a Commercial TDI monomers are produced in an 80:20 ratio of 2,4- and 2,6-isomers. For simplicity, only the 2,4-isomer is presented here.

picking up the film with a copper support grid. A series of four TDI polyurethane polymers were made by reacting toluene diisocyanate monomer with trifunctional poly(propylene oxide) polyols of different molecular weights (250, 700, 1500, and 3000 MW). The resultant TDI polyurethane polymers are identified here as T250, T700, T1500, and T3000, respectively.

The poly(ethylene oxide) polymer sample was obtained from Scientific Polymer Products (5 000 000 MW) and was melt-pressed into a disk for microtoming. The poly(propylene oxide) sample is an $-OH$ terminated, 700 MW polyol that was also used for the T700 polyurethane synthesis.

Solid samples were microtomed using a Reichert-Jung Fc4E with cryoattachment. Cryosections were typically cut at -120 °C and were transferred to bare copper support grids with an eyelash brush. The liquid polymer samples (B0 and the 700 MW PPO polyol) were prepared by dispersing the polymer in water and dropping a small quantity of this solution onto a thin, uniform, and X-ray transparent substrate (carbon-coated TEM grid for B0; 100 nm thick Si_3N_4 window for the poly(propylene oxide) polyol). Spectra were taken through uncovered substrate areas to correctly normalize for substrate absorption.

Molecular spectra were acquired in the gas phase by ISEELS and in the solid state by NEXAFS. The solid-phase sample of 2-propane diol was prepared by depositing a small drop of a 5% solution of the molecule in water onto a thin Si_3N_4 membrane. The water partially evaporated, although water has a small and featureless cross section at the C 1s core edge energies (270–320 eV). The molecule 2-propane diol was

purchased from Aldrich (99.5%). The spectra of ethyl *N*-phenyl carbamate and diisopropyl ether were published previously.⁷

2.2. NEXAFS Spectroscopy. NEXAFS spectra were recorded with the X-1A STXM at the National Synchrotron Light Source (NSLS) and with beamline 7.0 STXM at the Advanced Light Source. Spectra of these uniform samples were acquired with the X-ray beam defocused to a 5–15 μm diameter “donut” (the form of a defocused zone plate beam). The beam defocus is critical for distributing the X-ray dose over a suitably large volume of sample to reduce the rate of beam damage.⁵ Some of the spectra recorded at NSLS were acquired before a recent optics and monochromator upgrade.¹⁰ The energy resolution of these spectra is typically 0.15–0.30 eV fwhm, depending on the experimental conditions and the instrumentation on which the spectra were acquired. For energy scale calibration, CO_2 gas was added to the He purge in the microscope and the transmission spectrum of the mixture of the polymer and CO_2 gas was recorded. The energies of the $\text{CO}_2 \rightarrow \text{Rydberg}$ transitions from the high-resolution NEXAFS spectra of Ma et al.¹¹ were used to calibrate these spectra. These values are consistent with the calibrated electron energy loss spectra of Tronc et al.¹² The calibration is documented in the tables of spectral assignments.

2.3. Energy Loss Spectroscopy. ISEELS was used to record the C 1s core excitation spectrum of gaseous 2-propane diol and was used to record the previously published C 1s and O 1s core excitation spectra of ethyl *N*-phenyl carbamate and diisopropyl ether⁷ presented in this paper. These spectra were recorded using the McMaster gas-phase spectrometer,¹³ operated under inelastic scattering conditions under which electric dipole transitions dominate. The absolute energy scale was established by recording the spectrum of a stable mix of the analyte and a standard calibrant gas,¹⁴ as documented in the table of assignments. The energy resolution for the ISEELS spectra that are presented here is 0.5–0.7 eV fwhm.

The electron energy loss spectra of polymers⁶ were recorded in a scanning transmission electron microscope (STEM) (VG Microscopes model HB501, located at the National Institutes of Health) equipped with a field emission filament and a parallel EELS spectrometer (Gatan model 666).^{15,16} The electron dose was approximately 100 e^-/nm^2 (5 C/m^2) for the carbon K-edge and 400 e^-/nm^2 (20 C/m^2) for the oxygen K-edge spectra. The sample was cooled to ~ 100 K during acquisition. This system is capable of an energy resolution as good as 0.5 eV. However, to minimize radiation damage, spectra were acquired from 5 to 10 μm diameter regions with a defocused 100 nm beam rastered over the region of interest while simultaneously compensating for changes in the beam position by applying a synchronized voltage to the spectrometer drift tube. This “descan” procedure very likely degraded the instrumental resolution to something more than 1 eV. The potential for performing even higher resolution EELS spectroscopy of polymers may be realized soon. Some specialized existing TEM–EELS instruments have demonstrated 0.2–0.4 eV fwhm energy resolution for semiconductors¹⁷ and nickel aluminum intermetallics¹⁸ but not for polymers. The development of TEM monochromators capable of reaching 50 meV resolution is in progress.^{19,20} While higher energy resolution is possible in principle, the EELS spectra presented here represent the highest resolution EELS spectra of polyurethane polymers published to date.

3. Results and Discussion

3.1. Model Compound Studies. *3.1.1. Distinguishing TDI- and MDI-Based Polyurethanes.* Figure 1 presents the C 1s

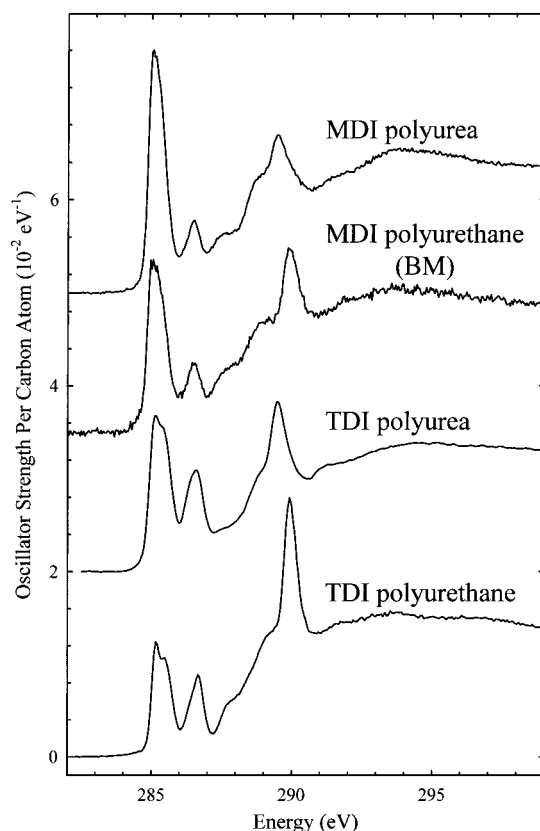


Figure 1. C 1s NEXAFS spectra of MDI polyurea, MDI polyurethane (BM), TDI polyurea, and the TDI polyurethane model polymers acquired by X-ray transmission and presented on an oscillator strength per carbon atom scale. See Chart 1 for polymer structures.

NEXAFS spectra of two MDI model polymers MDI polyurea and MDI polyurethane (BM) and the corresponding TDI models TDI polyurea and TDI polyurethane. Energies and spectral assignments are presented in Tables 1 and 2, and the polymer structures are presented in Chart 1.

The polyurethane and polyurea C 1s NEXAFS spectra have an intense C 1s(C–H) $\rightarrow 1\pi^*_{\text{C}=\text{C}}$ transition at 285.2 eV and a weaker C 1s(C–R) $\rightarrow 1\pi^*_{\text{C}=\text{C}}$ transition at 286.5 eV. (Note that the core level is indicated parenthetically before the arrow, while the nature of the upper level of a given transition is indicated as the final subscript. The C 1s(C–R) is the ring carbon to which the carbamate, urea, or isocyanate group is attached). The C 1s(C–R) $\rightarrow 1\pi^*_{\text{C}=\text{C}}$ feature is an electronic transition to the same optical orbital (i.e., the lowest unoccupied level in the π^* manifold common to all of the phenyl rings), except it originates from the phenyl ring carbon atom that is bonded to the amide group. The C 1s(C–R) $\rightarrow 1\pi^*_{\text{C}=\text{C}}$ transition is shifted to higher energy in part because the electron-withdrawing amide group increases the C 1s binding energy of this phenyl carbon and in part because of differences in the nature of the optical orbital and the nature of its response to core hole relaxation for states with core holes on C–H versus C–R carbons. This phenomenon is sometimes referred to as the “C–R shift”, and its magnitude depends on the identity of the R group of the “C–R” substituted moiety.

A similar C–H/C–R π^* energy splitting is observed in the TDI polymers. However, the intensity ratio of the C–R/C–H transitions is very different than for the MDI polymers. The pattern of C 1s(C–H) $\rightarrow 1\pi^*_{\text{C}=\text{C}}$ and C 1s(C–R) $\rightarrow 1\pi^*_{\text{C}=\text{C}}$ transitions in the 285–288 eV range of these spectra is the key to distinguishing MDI and TDI polyurethane polymers. This

TABLE 1: Energies (eV) and Assignments for the C 1s NEXAFS Spectra of MDI Polyurethanes (BM, B2, and B0) and MDI Polyurea

	model MDI polymers				assignment			
	BM	B2	B0	MDI polyurea	C-H	C-R	C=O	CH _x
1	285.18 ^a	285.18	285.18	285.18 ^a	1 $\pi^*_{C=C}$			
2	286.5	286.5	286.5	286.46		1 $\pi^*_{C=C}$		
3	287.6		287.4	287.4				C-H
4			288.1					C-H
5	289.0			288.7	2 $\pi^*_{C=C}$			
6		289.0	289.0		2 $\pi^*_{C=C}$			σ^*_{C-C}
7	290.94	289.94		289.5			$\pi^*_{C=O}$	
8 br	294.0			294.0	$\sigma^*_{C=C}$			σ^*_{C-O}
9 br				302	$\sigma^*_{C=C}$			

^a Calibrated by recording the transmission spectrum of an admixture of the polymer and CO₂ gas. Calibration: -7.62 eV relative to the center of the overlapping C 1s \rightarrow 3s($\nu=0$) and the C 1s \rightarrow 3s($\nu=1$) transitions in CO₂ (292.8 eV).¹¹

TABLE 2: Energies (eV) and Assignments for the C 1s NEXAFS Spectra of TDI Polyurea and TDI Polyurethane

	model TDI polymers		assignment			
	TDI polyurethane	TDI polyurea	C-H	C-R	C=O	CH _x
1	285.16 ^a	285.16 ^a	1 $\pi^*_{C=C}$			
2	285.44	285.44	1 $\pi^*_{C=C}$			
3	286.65	286.55		1 $\pi^*_{C=C}$		
4	287.5	287.8				
5	289.1	288.6	2 $\pi^*_{C=C}$			
6	289.94	289.5			$\pi^*_{C=O}$	
7	291.8	291.2				σ^*_{C-O}
8 br	294	294	$\sigma^*_{C=C}$			
9	298					
10 br	304	302	$\sigma^*_{C=C}$			

^a Calibrated by recording the transmission spectrum of an admixture of the polymer and CO₂ gas. Calibration: -7.64 eV relative to the center of the overlapping C 1s \rightarrow 3s($\nu=0$) and the C 1s \rightarrow 3s($\nu=1$) transitions in CO₂ (292.8 eV).¹¹

difference can be readily explained by examining the structure of the MDI and TDI polymers (see Chart 1). In the MDI polymers, each phenyl ring is bonded to one amide group and one methylene group; while in the TDI polymer, each phenyl ring is bonded to two amide groups and one methyl group. The C 1s spectra of xylenes demonstrate that the C-R shift due to methyl substitution is very small (~ 0.1 eV).²¹ Therefore, the methylene C-R shift can be neglected and only the amide C-R shifts are significant. In MDI-based polymers, one phenyl carbon will have the C-R shift and five phenyl carbons will not; in the TDI-based polymers, two phenyl carbons will have the C-R shift while four carbons will not. The observed spectral intensities of the C-H/C-R components agree semiquantitatively with this substitution counting prediction.

The C 1s(C-H) \rightarrow 1 $\pi^*_{C=C}$ transition in the MDI-based polymer spectra is nearly symmetrical within the experimental resolution, while this peak in the TDI-based polymers has two closely spaced components with the first peak slightly more intense than the second. The small splitting in the TDI C 1s(C-H) \rightarrow 1 $\pi^*_{C=C}$ transition reflects small shifts in the TDI phenyl ring carbon C 1s binding energies.

3.1.2. Distinguishing Urea and Carbamate Functionalities. The energy of the C 1s(C-R) \rightarrow 1 $\pi^*_{C=C}$ peak (near 286.6 eV) varies slightly between the urea and carbamate (urethane) polymer models. The largest difference is observed between the TDI polyurea and TDI polyurethane models. The C 1s(C-R) \rightarrow 1 $\pi^*_{C=C}$ feature is at lower energy and has a slightly different shape in the polyurea model than in the polyurethane model. In addition the C-H and C-R intensities differ, with an almost 30% increase in the C 1s(C-H) \rightarrow 1 $\pi^*_{C=C}$ peak intensity in the polyurea versus the polyurethane. A similar but smaller energy and shape difference is observed between the MDI polyurea and polyurethane models (which were recorded at lower resolution). These urea-carbamate shifts are consistent

with those observed for *N*-phenylurea and ethyl *N*-phenyl carbamate molecular models by C 1s ISEELS spectroscopy.⁷

These spectroscopic differences in the C 1s(C-R) \rightarrow 1 $\pi^*_{C=C}$ transitions between the spectra of polyurea and polyurethane are modest in comparison to the shift in the prominent C 1s(C=O) \rightarrow $\pi^*_{C=O}$ transition, which occurs at 289.5 eV in the urea-containing polymers and at 289.94 eV in the carbamate-containing polymers. This shift was predicted by gas-phase ISEELS results,⁷ extended Hückel MO (EHMO) calculations²² and high-quality ab initio⁸ calculations performed using the program GSCF3.²³ These calculations can be used to explore the relative contributions of valence delocalization and core binding energy shifts to this C 1s(C=O) \rightarrow $\pi^*_{C=O}$ transition shift. The valence electronic mixing shifts the carbamate $\pi^*_{C=O}$ optical orbital to lower energy relative to urea. This shift in $\pi^*_{C=O}$ energy is opposite to and smaller in magnitude than the shift in C 1s binding energy. The carbonyl C 1s binding energy shifts 0.76 eV between the urea and carbamate moieties (288.84 eV for polyurea; 289.60 eV for polyurethane).²⁴ Thus, the core binding energy shift is largely, but not solely, responsible for the difference in the C 1s(C=O) \rightarrow $\pi^*_{C=O}$ energies of the urea and carbamate.

In polymers containing phenyl groups, a C 1s(C-H) \rightarrow 2 $\pi^*_{C=C}$ transition is expected to occur at ~ 289 eV,²⁵ derived from the C 1s \rightarrow 2 $\pi^*(b_{2g})$ transition in benzene.²⁶ Above the carbonyl transition C 1s \rightarrow σ^* transitions are assigned in accordance with previous assignments.^{7,25}

3.1.3. Spectroscopy of the Polyether Component. Figure 2 presents the C 1s NEXAFS spectra of poly(ethylene oxide), poly(propylene oxide), and 2-propane diol (solid phase), in comparison to the ISEELS spectrum of 2-propane diol (gas phase). Energies and assignments of the polymer spectra are presented in Table 3 and that of the molecule 2-propane diol in Table 4.

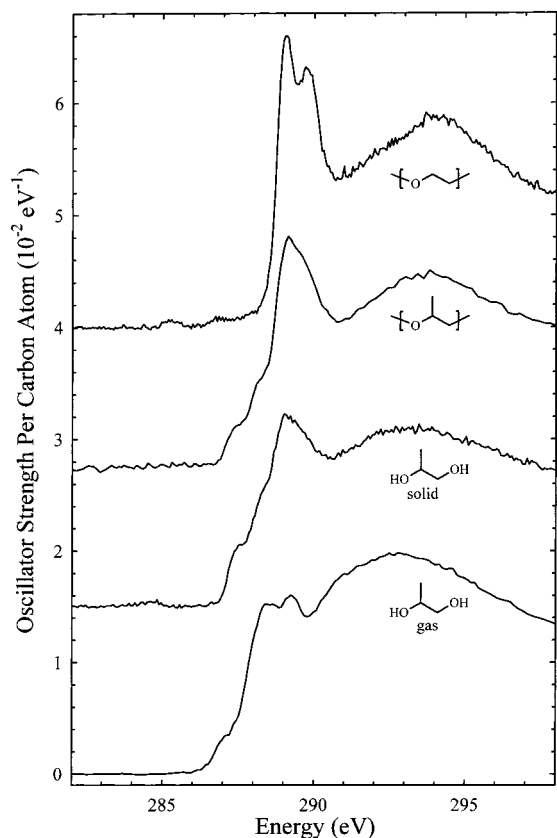


Figure 2. C 1s NEXAFS spectra of poly(ethylene oxide), poly(propylene oxide), and 2-propane diol (solid phase) acquired by X-ray transmission, in comparison to the C 1s ISEELS of 2-propane diol (gas phase). These spectra are presented on an oscillator strength per carbon atom scale.

TABLE 3: Energies (eV) and Assignments for the C 1s NEXAFS Spectra of Poly(ethylene oxide) and Poly(propylene oxide)

	polyethers		assignment	
	PEO	PPO	-CH _x -O	CH ₃
1		287.4		C-H
2		288.1		C-H
3	289.0 ^a	289.1 ^a	C-H	
4	289.7	289.6	C-H	
5	292.6			
6	294	293.8	σ* _{C-C}	σ* _{C-C}
7	305	305	σ* _{C-O}	σ* _{C-O}

^a Calibrated by recording the transmission spectrum of an admixture of the polymer and CO₂ gas. Calibration: PEO, -3.8 eV, and PPO, -3.7 eV, relative to the center of the overlapping C 1s → 3s(ν=0) and the C 1s → 3s(ν=1) transitions in CO₂ (292.8 eV).¹¹

The spectrum of poly(ethylene oxide) is quite simple, representing the contribution from the single CH₂ carbon atomic environment in the polymer, with a strong transition at 289 eV and a weaker but clearly resolved feature at 289.7 eV. In the C 1s NEXAFS spectrum of poly(ethylene oxide) published by Kikuma and Tonner²⁷ only one feature is observed at ~289 eV, but this difference is simply a function of the improved spectral resolution in the present work.

Except for chemical shifts, the general character of the low-energy spectral features in poly(ethylene oxide) are expected to be similar to those of polyethylene, where two low-energy features with a similar energy splitting are assigned as C 1s → C-H transitions of σ and π symmetry.^{28,29} In the solid phase, Rydberg transition contributions to these features are not

TABLE 4: Energies (eV) and Assignments for the C 1s NEXAFS Solid-Phase Spectrum of 2-Propanol and the C 1s ISEELS Gas-Phase Spectra of 2-Propanol and Ethylene Glycol

	2-propanol (solid)	2-propanol (gas)	assignment	
			-CH _x -O	CH ₃
1	287.5	287.0		C-H
2	288.3	288.3	σ* _{O-H}	C-H
3	289.1	289.24 ^a	C-H	
4	293.2	292.8	σ* _{C-O} /σ* _{C-C}	σ* _{C-C}

^a Calibration: 1.80(4) eV relative to C 1s → π*_{CO} transition in CO (289.40 eV).

expected,³⁰ although theoretical studies have proposed that there is a significant²⁹ or partial²⁸ Rydberg contribution to these features in polyethylene. The higher energy C 1s → σ*_{C-C} and C 1s → σ*_{C-O} transitions are assigned in accordance to previously published assignments on similar species.²²

The spectrum of poly(propylene oxide) is much more complex, since there are spectral contributions from three different carbon chemical environments (-CH₃, -CH₂-O-, and -O-CH-). There is an intense transition at ~289 eV, while at lower energy there are two shoulders on the rising edge (287.4 and 288.1 eV) of the spectrum. The two low-energy shoulders are expected to be C 1s → C-H transitions associated with the -CH₃ group. The intense transition at ~289 eV is tentatively assigned to C 1s → C-H transitions of the backbone carbon atoms at a similar energy as in poly(ethylene oxide).

The solid and gas phase C 1s spectra of 2-propane diol are included in this comparison because these molecules reproduce the carbon atom next-nearest-neighbor bonding environment present in poly(propylene oxide). It is generally believed that the local environment primarily determines the NEXAFS spectra of saturated hydrocarbons. Low-energy features (C 1s → C-H transitions) are observed at approximately the same energy in poly(propylene oxide) and in solid-phase 2-propane diol. We expect the spectrum of the 2-propane diol molecule to differ slightly from the poly(propylene oxide) spectrum because of contributions from a sharp C 1s → σ*_{O-H} transition observed at ~288 eV in alcohol species.^{31,32} The shift in the energy of the maximum of the overlapping σ*_{C-O} and σ*_{C-C} transitions is noteworthy (294 eV in the polymer; ~293 eV in the molecule). This difference may arise from "σ-conjugation"—interactions between adjacent monomer units that form a split band structure from a set of levels that would otherwise be degenerate at 293 eV in the isolated units.

The gas-phase C 1s ISEELS spectrum of 2-propane diol is very different from the spectrum of poly(propylene oxide) and the solid-phase spectrum of 2-propane diol. Part of the difference between the solid NEXAFS spectrum and the gas-phase ISEELS spectrum of 2-propane diol is due to differences in spectral resolution (0.3 vs 0.7 eV) as well as the expected attenuation of Rydberg transitions in the solid state.^{33,34} Rydberg transitions typically shift to higher energy in the solid state,³⁵ although shifts to lower energy are known for Rydberg transitions with large *n*.³⁴ The shift in the energy of the first transition in 2-propanol might suggest a Rydberg shift to higher energy in the solid state. However, it is difficult to make a firm conclusion on account of the strong overlap of the Rydberg and σ*/C-H transitions in 2-propane diol.

This comparison of gas and solid molecular and solid-phase polymer spectra demonstrates some of the challenges of applying "local" atomic neighbor models to interpreting polymer spectra, particularly for saturated species. This differs from the successful use of molecular models for interpreting the spectra of aromatic

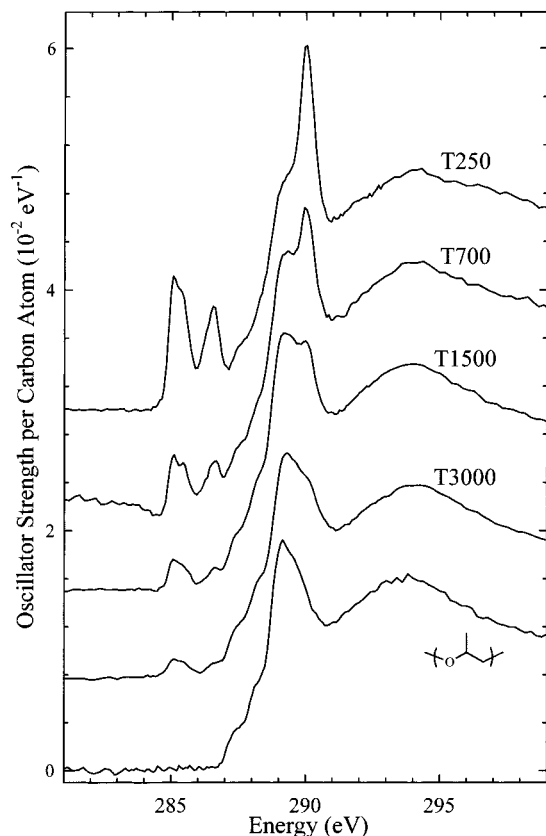


Figure 3. C 1s NEXAFS spectra of TDI polyurethanes made with 250, 700, 1500, and 3000 MW poly(propylene oxide) polyether polyols (labeled T250, T700, T1500, and T3000, respectively), compared to the C 1s NEXAFS spectrum of the 700 MW poly(propylene oxide) polyether polyol. These spectra were acquired by X-ray transmission and are calibrated with a precision of 30 meV.

polymers, particularly when the “spatial extent” of π^* delocalization in the polymer is properly accounted for in the molecular model structure.^{36,22} The effect of “ σ -delocalization” and the contentious issue of Rydberg transitions²⁹ in the core excitation spectroscopy of polymers deserve further experimental and theoretical study.

3.2. Polyether Concentration Dependence of NEXAFS Spectra of TDI Polyurethanes. Figure 3 presents the C 1s spectra of four TDI polyurethane polymers synthesized with poly(propylene oxide) polyether polyols of different molecular weight (250, 700, 1500, and 3000 MW), together with the C 1s spectrum of poly(propylene oxide). The only difference between these polymers is the molecular weight of the polyol reagent, which changes the effective ratio of the aromatic component to the polyether component in the polymer. As expected, there is a strong variation of the relative intensity of aromatic and polyether features as a function of the polyol molecular weight. The assignment of these spectra is similar to those of the TDI polyurethane model, above. The C 1s(C=O) \rightarrow $\pi^*_{C=O}$ transition is clearly visible in the polymers synthesized with the 250, 700, and 1500 MW polyols and can be identified as a very weak shoulder at 290 eV in the spectrum of the polymer made with the 3000 MW polyol. Figure 4 presents the spectrum of the carbamate component of the TDI polyurethanes made with the 1500 and the 3000 MW polyol, obtained by subtraction of the spectrum of poly(propylene oxide) scaled in proportion to the amount of polyether polyol in each species. Although noisy, all of the characteristic carbamate spectral features are detected, even when the carbamate linkage is a small fraction of the

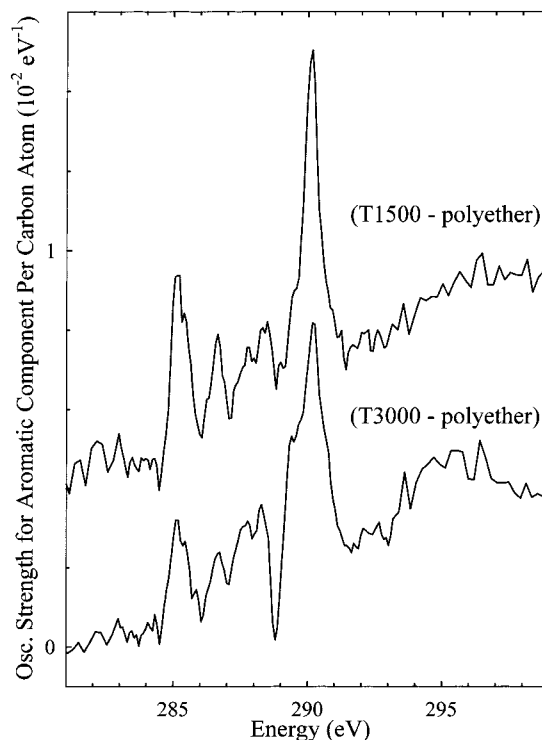


Figure 4. C 1s NEXAFS spectra of the carbamate component of TDI polyurethanes made with 1500 and 3000 MW poly(propylene oxide) polyether polyols (T1500 and T3000, respectively). The carbamate component was isolated by subtracting the poly(propylene oxide) spectrum from the polyurethane spectrum in proportion to the relative amount of poly(propylene oxide) present in the species.

polyurethane polymer. This sensitivity is important for the identification and quantification of urea and carbamate linkages in typical polyol-rich polyurethane materials.⁸

A second example of the effect of the poly(propylene oxide) concentration on C 1s NEXAFS spectra of MDI polyurethanes is presented below (section 3.3.1).

3.3. MDI Polyurethanes: Comparison of STXM–NEXAFS and TEM–EELS Methods. **3.3.1. C 1s Spectroscopy.** Figure 5 presents a comparison of the NEXAFS spectra of the MDI polyurethane models (BM, B2, and B0) (right panel) with the previously reported electron energy loss spectra (EELS) recorded in a transmission electron microscope (left panel).⁶ The gas-phase ISEELS of ethyl *N*-phenyl carbamate (top)⁷ and the solid-phase NEXAFS spectrum of 2-propane diol (bottom) are included for comparison. These MDI polymers only contain polyurethane linkages and have different proportions of what have been called “hard segment” (aromatic-rich polyurethane) and “soft segment” (polyether-rich) components. The structures of these polymers are presented in Chart 1.

The spectral assignments for the BM polymer (MDI polyurethane model) were discussed above (§3.1, 3.2). The B2 and B0 polymers differ from BM, since they include poly(propylene oxide) “soft-segment” copolymerized with the BM hard segment (see Chart 1). The assignments of the poly(propylene oxide) components of B2 and B0 follow from section 3.1.3, above. Since the electronic interaction between the “soft segment” poly(propylene oxide) and the “hard segment” MDI components is expected to be minimal, the spectra of the “mixed” component B2 and B0 polymers can be viewed as the sum of the soft and hard segment contributions.

The comparison of higher resolution NEXAFS spectra (0.15–0.25 eV fwhm) and lower resolution TEM–EELS (~1 eV

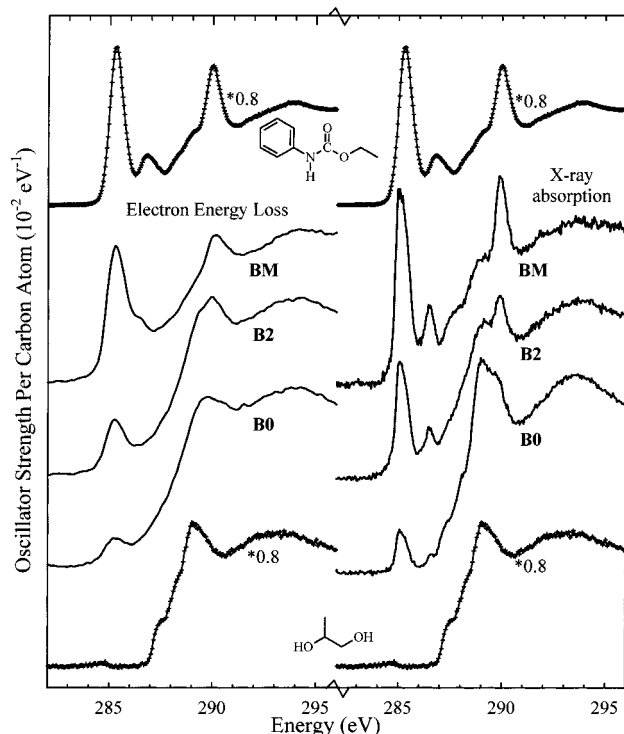


Figure 5. C 1s NEXAFS spectra of the MDI polyurethane models B0, B2, and BM, acquired by X-ray transmission (right panel) in comparison to the C 1s EELS of these MDI polyurethane models acquired in a transmission electron microscope (left panel).⁶ These spectra are compared to the C 1s gas-phase (ISEELS of ethyl *N*-phenyl carbamate (top trace) and the C 1s solid-phase NEXAFS spectrum of 2-propane diol (bottom trace). The molecular spectra are presented as lines with data points, while the polymer spectra are presented as solid lines.

fwhm)⁶ and ISEELS (0.7 eV fwhm) spectra clearly illustrates the improvement in chemical sensitivity with higher spectral resolution. While similar spectral trends can be discerned in both the EELS and NEXAFS data, the differences are clearer with higher energy resolution and the features can be assigned with more confidence. For example, the C 1s(C=O) \rightarrow $\pi^*_{C=O}$ transition is resolved in all three NEXAFS spectra, whereas it is only just visible in the BM and B2 EELS spectra. The ability to distinguish such features is not just a matter of convenience but is *essential* in the application of polymer NEXAFS to component quantification in polyurethanes,⁸ especially in samples with a high polyether concentration.

3.4. O 1s Spectroscopy. Figure 6 presents the O 1s NEXAFS spectra of the MDI polyurethane polymers BM and B2 (right panel), in comparison to the previously published C 1s EELS spectra of MDI polyurethane polymers BM, B2, and B0 (left panel),⁶ and the O 1s ISEELS spectra of ethyl *N*-phenyl carbamate (top) and diisopropyl ether (bottom).⁷ Table 5 lists the energies and spectral assignments for the O 1s NEXAFS spectra of B2 and B0. These are based on previous assignments of lower resolution EELS spectra of these polymers and ISEELS spectra of molecular models.^{7,6}

There are two prominent differences between the O 1s EELS and the NEXAFS spectra. In the higher energy resolution NEXAFS spectra, the O 1s(C=O) \rightarrow $\pi^*_{C=O}$ transition is sharp and clearly resolved, even better than in the gas-phase ethyl *N*-phenyl carbamate model spectrum. The corresponding transition in the EELS polymer spectrum is not resolved. This is in part because of the poorer spectral resolution of the O 1s EELS spectra, but the effect of beam damage on the polymer O 1s

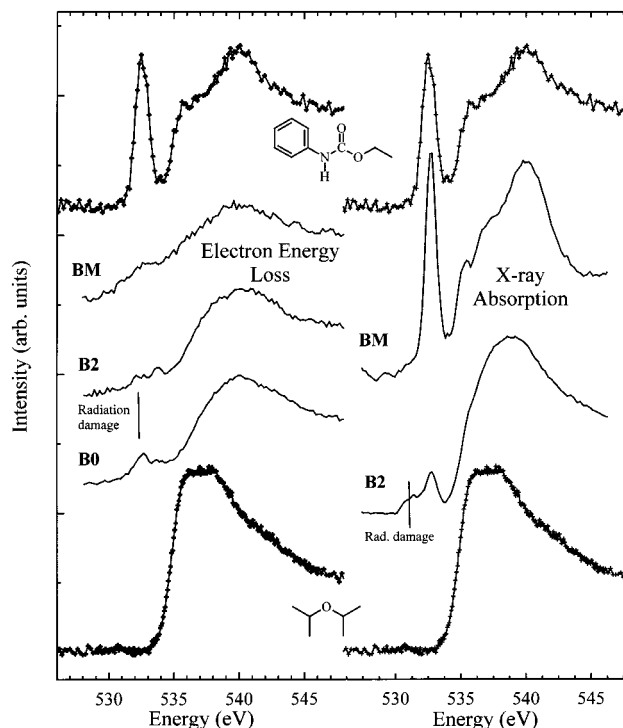


Figure 6. O 1s NEXAFS spectra of the MDI polyurethane models BM and B0, acquired by X-ray transmission (right panel) in comparison to the O 1s EELS of MDI polyurethane models BM, B2, and B0, acquired in a transmission electron microscope (left panel).⁶ These spectra are compared to the O 1s gas-phase ISEELS of ethyl *N*-phenyl carbamate (top trace) and diisopropyl ether (bottom trace). The molecular spectra are presented as lines with data points, while the polymer spectra are presented as solid lines.

TABLE 5: Energies (eV) and Assignments for the O 1s NEXAFS Spectra of MDI Polyurethanes BM and B2

	model MDI polymers		assignment		
	BM	B2	C=O	O-R	other
1		530.8			O ₂ (?)
2		531.4	$\pi^*_{C=O}$?
3	532.7	532.7		$\pi^*_{C=O}$	
4	535.4	535.6 (sh)		$\pi^*_{C=O}$	
5	537			σ^*_{C-O}	
6	540	539		σ^*_{C-O}	

spectra may also be significant. A recent study of the X-ray radiation damage rates for a large series of polymers indicated that unsaturated polymers such as poly(propylene oxide) and carbonyl functional groups are particularly sensitive to radiation damage.³⁷ Given this constraint, it is difficult to get higher quality O 1s EELS spectra for polyurethanes.

In addition to the main O 1s(C=O) \rightarrow $\pi^*_{C=O}$ transition, the O 1s(O-R) \rightarrow $\pi^*_{C=O}$ transition is resolved at 535.4 eV. This feature originates from delocalization of the $\pi^*_{C=O}$ density onto the -O-R oxygen atom. The presence of this O 1s(O-R) \rightarrow $\pi^*_{C=O}$ transition in carbamate had been predicted to be key to distinguishing between urea and carbamate linkages.⁷

The O 1s spectrum of MDI model B2 illustrates the influence on the spectrum of increased concentration of poly(propylene oxide); the contributions of the polyether increase greatly relative to those from the carbonyl of the carbamate. The ISEELS spectrum of diisopropyl ether is an excellent model for this environment, since it reflects the *next-neighbor* atomic environment of the oxygen atom. The O 1s spectrum of diisopropyl ether consists of O 1s \rightarrow σ^*_{C-O} transitions. These σ^*_{C-O} transitions are responsible for the broad spectral intensity at 539

eV in the spectrum of B2. The signal around 531 eV in the EELS of B2 and B0, as well as in the NEXAFS of B2, is most likely a spectral feature of a radiation damage product.

4. Summary

NEXAFS microscopy can be a useful probe for microanalysis of polyurethane polymers if it can distinguish urea and carbamate linkages, quantify the polyether content, and identify the type of diisocyanate used (MDI versus TDI). All of these capabilities have been demonstrated in the present work. In addition the spectral origin of the speciation capability is identified. The C 1s and O 1s NEXAFS spectroscopy of the pure components of complex polyurethane polymers have been presented and discussed. Differences in phenyl ring substitution cause substantial differences in C 1s $\rightarrow 1\pi^*_{C=C}$ transition energies and character. These differences provide a mechanism for distinguishing MDI- and TDI-based polyurethane polymers. On the basis of shifts in the C 1s(C-R) $\rightarrow 1\pi^*_{C=C}$ and the C 1s(C=O) $\rightarrow \pi^*_{C=O}$ transition energies, NEXAFS provides an unambiguous spectroscopic fingerprint for distinguishing urea and carbamate (urethane) linkages in polyurethane polymers. The carbonyl transition is visible even when the polyether concentration in the polymer is high. This level of sensitivity will be vital to quantitative chemical studies of complex polyurethanes,⁸ where there can be 70% or more polyether and other species present. O 1s NEXAFS spectra provide a probe complementary to C 1s spectroscopy for studying the links between chemistry and microstructure of polyurethanes.

Acknowledgment. Research was carried out at the National Synchrotron Light Source (NSLS) at Brookhaven National Laboratory (supported by the U.S. Department of Energy, Division of Materials Sciences and Division of Chemical Sciences under Contract DE-AC02-98CH10886) and at the Advanced Light Source (ALS) at Lawrence Berkeley National Laboratory (supported by the U.S. Department of Energy, Office of Energy Research, Office of Basic Energy Sciences, Materials Sciences Division under Contract DE-AC03-76SF00098). Data were recorded using the Stony Brook STXM microscope at the NSLS, the BL7.0 STXM microscope at the ALS, and the ISEELS spectrometer at McMaster University. The Stony Brook STXM was developed by the group of J. Kirz and C. Jacobsen, with support from the U.S. Department of Energy, Office of Biological and Environmental Research (Contract DE-FG02-89ER60858) and the National Science Foundation (Grant DBI-9605045). The zone plates were developed by S. Spector and C. Jacobsen of Stony Brook and Don Tennant of Lucent Technologies Bell Labs, with support from the NSF under Grant ECS-9510499. The ALS STXM was developed by T. Warwick (ALS), B. Tonner (UWM), and collaborators, with support from the U.S. DOE. H. Ade and A.P. Smith are supported by NSF Young Investigator Award (DMR-9458060). R. Herrington helped prepare the polyurethanes with different molecular weight polyols. A.P. Hitchcock is supported by NSERC strategic and research grants. We thank L. Ennis for assisting with the diol measurements.

References and Notes

(1) Herrington, R. *Flexible Polyurethane Foams*, 2nd ed.; The Dow Chemical Company: Midland, MI, 1997.

- (2) Hitchcock, A. P.; Ade, H. W.; Smith, A. P.; Urquhart, S. G.; Rightor, E. G.; Lidy, W. Manuscript in preparation.
- (3) Ottensmeyer, F. P. *J. Ultrastruct. Res.* **1984**, *88*, 121–134.
- (4) Egerton, R. F. *Electron Energy Loss Spectroscopy in the Electron Microscope*; Plenum Press: New York, 1986.
- (5) Rightor, E. G.; Hitchcock, A. P.; Ade, H.; Leapman, R. D.; Urquhart, S. G.; Smith, A. P.; Mitchell, G.; Fisher, D.; Shin, H. J.; Warwick, T. *J. Phys. Chem. B* **1997**, *101*, 1950–1961.
- (6) Urquhart, S. G.; Hitchcock, A. P.; Leapman, R. D.; Priester, R. D.; Rightor, E. G. *J. Polym. Sci., Part B: Polym. Phys.* **1995**, *33*, 1593–1602.
- (7) Urquhart, S. G.; Hitchcock, A. P.; Priester, R. D.; Rightor, E. G. *J. Polym. Sci., Part B: Polym. Phys.* **1995**, *33*, 1603–1620.
- (8) Urquhart, S. G.; Hitchcock, A. P.; Smith, A.; Ad, H. W.; Lessard, B.; Lidy, W.; Rightor, E. G.; Mitchell, G. E. *J. Electron Spectrosc. Relat. Phenom.*, in press.
- (9) Christenson, C. P.; Harthcock, M. A.; Meadows, M. D.; Spell, H. L.; Howard, W. L.; Creswick, M. W.; Guerra, R. E.; Turner, R. B. *J. Polym. Sci., Part B: Polym. Phys.* **1986**, *24*, 1401–1439.
- (10) Rarback, H.; Buckley, C.; Ade, H.; Camilo, F.; DiGennaro, R.; Hellman, S.; Howells, M.; Iskander, N.; Jacobson, C.; Kirz, J.; Krinsky, S.; Lindaas, S.; McNulty, I.; Oversluisen, M.; Rothman, S.; Sayre, D.; Sharnoff, M.; Shu, D. *J. X-Ray Sci. Technol.* **1990**, *2*, 274–296.
- (11) Ma, Y.; Chen, C. T.; Meigs, G.; Randall, K.; Sette, F. *Phys. Rev. A* **1991**, *44*, 1848–1858.
- (12) Tronc, M.; King, G. C.; Read, F. H. *J. Phys. B: At. Mol. Phys.* **1979**, *12*, 137–157.
- (13) Hitchcock, A. P. *Phys. Scr.* **1990**, *T31*, 159–170.
- (14) Sodhi, R. N. S.; Brion, C. E. *J. Electron Spectrosc.* **1984**, *34*, 363.
- (15) Krivanek, O. L.; Ahn, C. C.; Keeney, R. B. *Ultramicroscopy* **1987**, *22*, 103.
- (16) Leapman, R. D.; Andrews, S. B. *J. Microsc.* **1991**, *161*, 3.
- (17) Batson, P. E. *Electron Energy Loss Studies in Semiconductors. In Transmission Electron Energy Loss Spectrometry in Materials Science*; Disko, M. M., Ahn, C. C., Fultz, B., Eds.; The Minerals, Metals and Materials Society: Warrendale, PA, 1992; p 217.
- (18) Muller, D. A.; Batson, P. E.; Silcox, J. *Phys. Rev. B* **1998**, *58*, 11970–11981.
- (19) Kruit, P. *Electron Microsc. Anal.* **1997**, *153*, 269–272.
- (20) Mook, H. W.; Kruit, P. *Electron Microsc. Anal.* **1997**, *153*, 81–84.
- (21) Eustatiu, I. G.; Huo, B.; Urquhart, S. G.; Hitchcock, A. P. *J. Electron Spectrosc. Relat. Phenom.* **1998**, *94*, 243–252.
- (22) Urquhart, S. G. *Core Excitation Spectroscopy of Molecules and Polymers*. Ph.D. Thesis, McMaster University, Hamilton, Ontario, Canada, 1997.
- (23) Kosugi, N.; Kuroda, H. *Chem. Phys. Lett.* **1980**, *74*, 490.
- (24) Beamson, G.; Briggs, D. *High-resolution XPS of organic polymers: the Scientia ESCA300 database*; John Wiley & Sons Ltd: New York, 1992.
- (25) Hitchcock, A. P.; Urquhart, S. G.; Rightor, E. G. *J. Phys. Chem.* **1992**, *96*, 8736–8750.
- (26) Horsley, J. A.; Stöhr, J.; Hitchcock, A. P.; Newbury, D. C.; Johnson, A. L.; Sette, F. *J. Chem. Phys.* **1985**, *83*, 6099–6107.
- (27) Kikuma, J.; Tonner, B. P. *J. Electron Spectrosc. Relat. Phenom.* **1996**, *82*, 53–60.
- (28) Stöhr, J.; Outka, D. A.; Baberscke, K.; Arvanitis, D.; Horsley, J. A. *Phys. Rev. B* **1987**, *36*, 2976–2979.
- (29) Bagus, P. S.; Weiss, K.; Schertel, A.; Wöll, Ch.; Braun, W.; Hellwig, C.; Jung, C. *Chem. Phys. Lett.* **1996**, *248*, 129–135.
- (30) Hitchcock, A. P.; Newbury, D. C.; Ishii, I.; Stöhr, J.; Horsley, J. A.; Redwing, R. D.; Johnson, A. L.; Sette, F. *J. Chem. Phys.* **1986**, *85*, 4849–4862.
- (31) Urquhart, S. G.; Hitchcock, A. P. Unpublished data.
- (32) Ishii, I.; Hitchcock, A. P. *J. Electron Spectrosc. Relat. Phenom.* **1988**, *46*, 55–84.
- (33) Xiong, J. Z.; Jiang, D. T.; Liu, Z. F.; Baines, K. M.; Sham, T. K.; Urquhart, S. G.; Wen, A. T.; Tyliczszak, T.; Hitchcock, A. P. *Chem. Phys.* **1996**, *203*, 81–92.
- (34) Robin, M. B. *Higher Excited States of Polyatomic Molecules*; Academic Press: Orlando, FL, 1985; Vol. III.
- (35) Rühl, E.; Hitchcock, A. P.; Morin, P.; Lavollee, M. *J. Chim. Phys. (Paris)* **1995**, *92*, 521.
- (36) Urquhart, S. G.; Hitchcock, A. P.; Smith, A. P.; Ade, H.; Rightor, E. G. *J. Phys. Chem. B* **1997**, *101*, 2267–2276.
- (37) Coffey, T. S. M.Sc Thesis, North Carolina State University, Raleigh, NC, 1998.